

NOTATION

D_t) tube diameter, m; f) active grating cross section, %; G_s) specific charge of disperse material, $\text{kg}/(\text{m}^2 \cdot \text{sec})$; H) distance from the gas distribution grating to the middle of the calorimeter, m; l) length of the heat transfer section, m; $\overline{Nu}_t = \alpha_K l / \lambda$) Nusselt number, describing external heat transfer on the plate; $Re_t = wl / \nu$) Reynolds number for the plate; Pr) Prandtl number; w) speed of filtration of gas, computed from the empty channel cross section, m/sec; α) total heat transfer coefficient, $\text{W}/(\text{m}^2 \cdot \text{K})$; α_K) convection-conduction heat transfer coefficient, $\text{W}/(\text{m}^2 \cdot \text{K})$; λ) thermal conductivity, $\text{W}/(\text{m} \cdot \text{K})$; ρ) bed density, kg/m^3 ; K) kinematic viscosity, m^2/sec . The subscripts are: t) tube; v) convective-conductive; r) radiative.

LITERATURE CITED

1. V. K. Maskaev, A. P. Baskakov, A. G. Usol'tsev, and I. V. Ivanov, *Inzh.-fiz. Zh.*, **57**, No. 5, 762-767 (1989).
2. A. A. Zhukauskas, *Convective Heat Transfer in Heat Exchangers* [in Russian], Moscow (1982).

RESONANCE REGIMES IN NONUNIFORM MOIST VIBRATION-FLUIDIZED BEDS

A. F. Ryzhkov and V. A. Mikula

UDC 536.24:66.096.5

Actual and approximate rheodynamic characteristics are presented for nonuniform, moist vibration-fluidized beds. Good correlation is obtained between calculated dynamic properties and experimental data.

We will examine several practically important relationships for specific cases which combine the presence of extremal (resonance) dependence of the pulsation characteristics on a spatial parameter H of an oscillating system and the frequency ω of the forced motions.

Introduction. The application of a combined method of fluidization makes it possible to input industrially required gaseous reagents and simultaneously to control the motion of a vibrating bed, mainly by increasing the working porosity of the charge. A large number of empirical correlations (see [1-3]) are used for describing the expansion of a vibration-fluidized bed. We applied Richardson's and Zacey's formula for our data [4] and were able to calculate the expansion of a homogeneous vibrating bed with thinly dispersed materials for a given aeration rate.

During the investigation of pressure oscillations in a vibrating bed it was established [5-7] that adding a steady gas flow to the vibration-expanded bed had no practical effect on the resonance character of the vibration liquefaction. The average pressure drop ΔP in the bed for $W \ll 1$ corresponds to vibration liquefaction, but for $W \geq 1$ to a fluidized bed. The frequency spectrum of the pressure pulsations for combined fluidization becomes bimodal with peaks at the vibration frequency and the resonant frequency of the fluidized bed. Thus, the fluidized bed is a limiting case of a vibration-fluidized bed, in which the pulsation has only low-frequency components, while the forced high-frequency oscillators are almost totally damped. A similar case was investigated experimentally and theoretically by Rietema [8] by submersing a vibrating screen in a fluidized bed. When the whole gas-dispersing lattice was vibrated, the increase of the fluidization number to $W = 5-10$ caused a 50-70% erosion of the pulsation amplitude at the applied frequency. Here the energy of the remaining pulsations still exceeded the level of pulsations in the fluidized bed by an order of magnitude. From this it follows that the expansion of the bed is a basic factor through which the gas flow affects the bed dynamics.

S. M. Kirov Ural Polytechnic Institute, Sverdlovsk. Translated from *Inzhenerno-fizicheskii Zhurnal*, Vol. 61, No. 5, pp. 782-789, November, 1991. Original article submitted October 16, 1990.

In processing the dispersed material, the problem arises of fluidizing elements of the bulk material with a wide range of dimensions (0-50 mm and larger) and densities (0.1-10 tons/m³). Even the first investigations into vibration-liquefaction showed [9] that applying vibration could produce the same good fluidization for both fine and coarse particles, including cases in which there was no gas flow. In the last case, fluidizing heterogeneous particles was most successful in a vibration-fluidized bed with a dispersed fine carrier. Here the equivalent diameter of the interstitial channel is determined mainly by the fine fraction, which creates the necessary dynamic conditions in the vibrating mixture for suspending the granules in forms characteristic of finely dispersed vibrating beds, with insignificant corrections [10]. These forms create all the necessary conditions for the maximum heat and mass transfer, which was observed experimentally [11].

During the vibrational processing, the initial mixture undergoes a series of transitions, which are characterized by the usual interchange of dual-phase (liquid-particle and gas-particle) and triple-phase (liquid-gas-particle) states. Purely filtration and nonresonant fluidization regimes are developed for liquid-saturated systems [13]. A gas-saturated bed is characterized by the development of resonant effects and the intensive motion of material almost to a complete outflow of the vapor-gas mixture from the pores of the vibrating charge with the coarsening of the dispersed composition as a result of spontaneous granulation [4, 6, 13-15].

I. Computational Equations. We will examine the simplest type of vibration-fluidization of a binary mixture of particles, which differ greatly in density, dimensions, and porosity. For definiteness, we will assume that the fine particles (f), which have a diameter d , are nonporous, and the coarse (c) with a diameter D (clusters, granules, clinkers, products, etc.) have a dynamic internal porosity $\varepsilon_{c\omega}$. The latter includes only the aerated part of the internal pores ε_c , which has the possibility of exchanging gas with the interparticle space during the vibration period. The total "connection" of the internal pores to the dynamic process occurs if the effective depth of the filtration penetration of the gas in the pores of the granule S is larger than its transverse diameter D . The basic characteristics of such a mixture are as follows:

1. The volume concentration c and the density τ of coarse and fine components and the bed porosity:

$$c_c + c_f = 1; \tau_c + \tau_f = 1 - \varepsilon; \varepsilon = \varepsilon_0 + \tilde{\varepsilon}_c, \quad (1)$$

where ε_0 and $\tilde{\varepsilon}_c$ are the "external" (intergranular) and "internal" (intragranular) porosity in the bed.

2. The density of the mixture:

$$\rho_b = \rho_f(1 - \varepsilon)(1 - c_c(1 - \rho_c/\rho_f)). \quad (2)$$

3. The effective diameter of the particles d^* , which creates the hydraulic resistance of the bed equivalent to the initial mixture:

$$d^* = dD/(c_c d + c_f D). \quad (3)$$

According to general recommendations [16] the particle dimension d^* in the mixture is found as a harmonically averaged quantity.

4. The effective porosity of the mixture in the dynamic state:

$$\varepsilon_{c\omega}^* = \varepsilon_0 + \tilde{\varepsilon}_{c\omega} \leq \varepsilon, \quad (4)$$

where $\tilde{\varepsilon}_{c\omega} = \alpha \varepsilon_c (1 - \varepsilon) c_c / (1 - \alpha \varepsilon_c)$ is the dynamic connected "internal" porosity of the coarse grains in the bed, which can be computed from the actual porosity of these grains ε_c and the permeability coefficient $\alpha \approx (2S/D)^3$. Here the parameter S is the path traversed by the gas in a half-period of the vibration and has the sense of the slippage of the phases in the model of a dual-phase, dual-velocity continuum. According to [17], the value of S is determined by the vibration velocity V_v , the velocity relaxation time of the phases τ_v and the dimensionless oscillation amplitude of the dispersed phase η_x , which is found by solving the problem of the vibrating bed dynamics:

$$S = \eta_x V_v \tau_v. \quad (5)$$

TABLE 1. Classification of Vibrating Beds

Categories of vibrating beds	Thinly dispersed dusts (T)		Fine dispersions (F)	Intermediate grains (IG)	Large grains (L)	Spheres and lumps (SPH)
Particle diameter, μm	0.1-20	20-50	50-200	200-500	500-1500	1500
Bed group according to Geldart [25]	C	A	B	B	D	D
Relative oscillation frequency θ_v	10^{-5} - 10^{-3}	10^{-3} -0.33	0.33-1.7	1.7-10	10-100	100
Relative slippage depth of phases S/d	10^{-1}	10^0	10^1	10^2	10^3	10^3

If a grain of the coarse fraction D is a conglomerate of fine particles d, the value of S is easily evaluated as a function of the classes of vibrating dispersed material. The order of magnitude of the particle dimensions is recorded for materials of average density $\rho_f = 2.6 \cdot 10^3 \text{ kg/m}^3$, which vibrate under normal conditions at a frequency of $20 \pm 5 \text{ Hz}$.

As can be seen from Table 1, conglomerates which consist of thinly dispersed particles of class C can be considered practically unfluidizable ($\epsilon_{c\omega} \approx 0$). If the granules are based on dispersed fine particles or coarser particles, the entire porosity $\bar{\epsilon}_c$ is added to the external porosity ϵ_0 and $\epsilon_{\omega} \equiv \epsilon$.

The "external" porosity ϵ_0 is formulated from the effect of structure-forming factors in the system. In the case of gas flow, this function has the form

$$\epsilon_0 = \begin{cases} \epsilon_v & \text{for } W = 0 - 1, \\ ((v/v_t)^{1/n}) & \text{for } W > 1. \end{cases} \quad (6)$$

A triple-branched approximation can be used for a binary layer:

$$\epsilon_0 = \begin{cases} \epsilon_f^0 g_f / (1 - \epsilon_f g_c) & \text{for } g_f > g_c, \\ \epsilon^{\text{min}} & \text{for } g_f \sim g_c, \\ \epsilon_c^0 g_c / (1 - \epsilon_c g_f) & \text{for } g_c > g_f. \end{cases} \quad (7)$$

According to this description, at small concentrations the addition of "external" porosity to the mixture is determined by the porosity of the dominant fraction in the absence of impurities, but in the saturation range, it can be taken equal to the minimum working porosity of the mixture (see Fig. 2a"), according to which our data and data from the literature [18] is $\approx 0.4-0.45$.

For a moist bed, the basic equations (1)-(4) retain their previous form, if instead of the subscripts c and f we use p (particle), g (granule), d (initial material) and l (liquid).

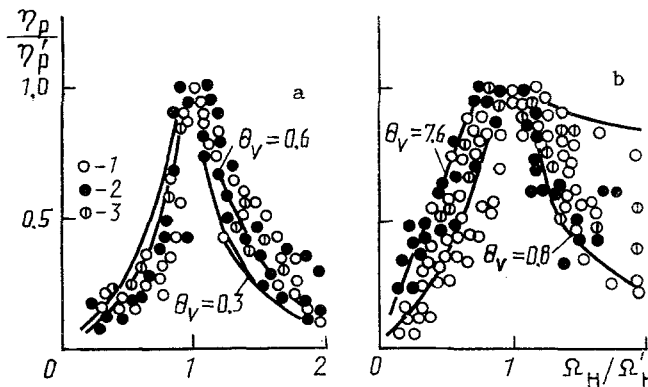


Fig. 1. Resonance curves of gas pressure pulsations: 1, 2) g_c , $U = \text{var}$; 3) $W = \text{var}$ [22]; a) $g_c = 0-60\%$, $U = 0-0.3\%$, $W = 0-0.5$; b) $g_c = 70-100\%$, $U = 0.9-10\%$, $W = 1-7$; curves are calculated according to (8).

The quantity α has its previous meaning and depends on the moisture content of the vibrating bed. For example, in the case examined in [15] (corundum, $d = 70$ mm, $f = 20$ Hz, $A_V = 3$ mm) the internal porosity of the granules from calculations affects the dynamic process for $U < 2\%$ ($\alpha \geq 1$) and becomes insignificant ($\alpha \sim 0$) for $U = 2-14\%$.

Introducing the effective characteristics of the vibrating mixture makes it easy to use the concepts [17] of a vibrating bed as a dual-velocity, dual-phase continuum, whose dynamics are described by the equation

$$D_{tt}p - a_0^{*2}(1 + \tau_v^* D_t) D_{xx}p = 0, \quad (8)$$

where

$$a_0^* = \frac{P_0}{\rho_{f,p}(1-\varepsilon)\varepsilon^*(1-c_c(1-\rho_{c,l}/\rho_{f,p}))},$$

$$\tau_v^* = \frac{\rho_{f,p}\varepsilon^{*3}d^{*2}(1-\varepsilon)(1-c_c(1-\rho_{c,l}/\rho_{f,p}))}{150(1-\varepsilon^*)^2\mu}$$

are the effective values of the equilibrium sound speed a_0 and the velocity relaxation time τ_v in the mixture. The rheodynamic model of a vibrating bed used in [17] can be rewritten in an analogous manner:

$$\dot{X}^* + \omega_0^{*2}(\tau_v^* \dot{X}^* + X^*) = \ddot{X}_v, \quad p = \rho_c^* H \omega_0^{*2}(X^* + \tau_v^* \dot{X}^*), \quad (9)$$

where $X^* = (2/\pi)(\varepsilon_0^* H_0 - \varepsilon^* H)$ is the dynamic structural deformation of the vibrating bed, and $\omega_0^* = (\pi/2)(a_0^*/H)$ is the characteristic frequency of elastic oscillations of the mixture.

II. Discussion and Experimental Verification. For $c_c = 0$, Eqs. (8) and (9) are identical to the initial equations [17]. Introduction of coarse additives changes the volume of the gas phase and the inertia of the bed. When light nonporous additions are processed ($\rho_c < \rho_f$, and $\varepsilon_c = 0$), both factors act in the same direction and the characteristic frequency ω_0^* increases dramatically. If the additives have open internal porosity ($\varepsilon_c > 0$), the factors can compensate each other and the change in ω_0^* will not be that large as c_c increases. If the bed is loaded with heavy particles ($\rho_c > \rho_f$), ω_0^* decreases. However, the trajectory of the additive grains in this case can differ significantly from the motion of the filler [19].

If the vibration liquefaction occurs via a rigid shock, repeated inertial surges of the additives and retention of the fines in the base due to aerodynamic forces are accompanied by fractionation of the mixture with complete loss of the additives from the bottom of the bed.

Decreasing the fractionation rate and the transition to a homogenization of the mixture occur when the moving-bed regime is replaced by the suspended regime (which was noted by Volik [20]) and also when enough heavy particles are introduced into the bed so that the density difference of vibrating fines becomes insignificant ($\rho_c/\rho_f > 6$ [10]).

Experiments were conducted in a vertically vibrating Plexiglas unit with an internal diameter of 113 mm. The amplitude of the pressure pulsations of the gas δP_g at the bottom of the apparatus, the reduced mass M , and the height H of the bed were fixed. The working medium was a mixture of nonporous particles of identical density and a moistened monofraction charge of the same materials [13]. The gas pressure pulsations were recorded by standard techniques [7].

Dimensionless resonance curves of the pulsation amplitudes of the gas pressure, obtained in the tests as a function of the vibration frequency, agree well with the calculated results for all bed compositions and moisture contents (Fig. 1). Data [21] on the dynamics of vibration-fluidized beds conform to analogous functions.

Analysis of the dependence of the pressure resonant pulsations and the corresponding vibration-liquefaction frequencies shows (Fig. 2a) that for small concentrations of the coarse or fine additives, distortions in the bed structure in the interphase region can be neglected, and the porosity of the "pure" components (ε_f^0 and ε_c^0 , respectively) can be used in the calculations. At intermediate concentrations, agreement with experiment occurs with the use of approximation $\varepsilon = \varepsilon^{\min}$. It should be noted that the extrema in the curves $\varepsilon(g_c)$ and $\delta P'(g_c)$ do not coincide, because $\delta P'$ is affected by both porosity change and a general

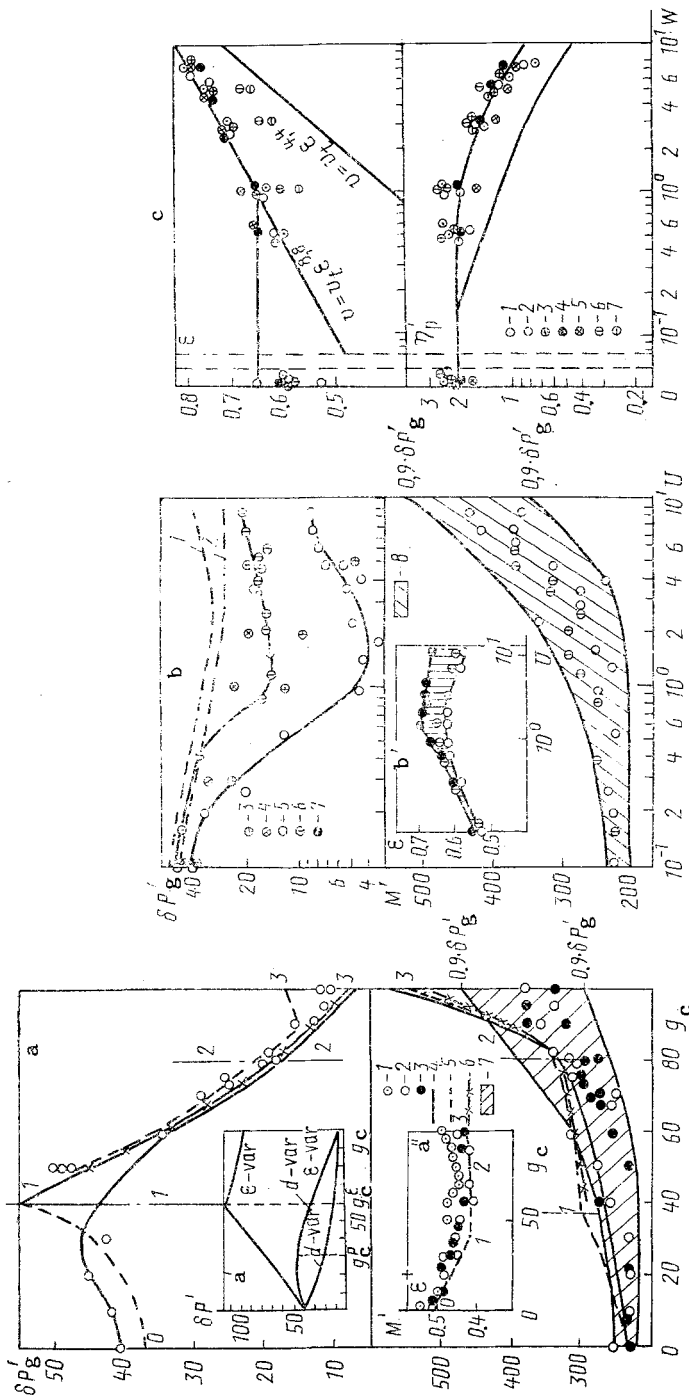


Fig. 2. Resonant pressure pulsations (kPa) and specific mass (kg/m^2) of the vibrating layer as a function of the system parameters: a, a' , a'' : 1) $k = 0$; 2) $k = 3.2$; 3) $k = 5.6$; solid curves calculated using (8); dashed curves calculated using (9); 4) ϵ from experiment; 5, 6) ϵ from (7); 7) region of $(0.9-1)\delta P_g'$; b and b': 1, 2) $\delta P_{\text{tot}}'$ [16]; 3-6) $\delta P_g'$; 1, 3) $k = 4$; 2, 4, 6) $k = 5.6$; 7) $k = 0$; $f = 20$ Hz, corundum; 8) range of $(0.9-1)\delta P_g'$; c: 1) $f = 20$ Hz, $k = 3$; 2) $f = 20$ Hz, $k = 5$; 3) $f = 20$ Hz, $k = 7$; 4) $f = 20$ Hz, $k = 10$; 5) $f = 20$ Hz, $k = 15$; 6) $f = 30$ Hz, $k = 7$; 7) $f = 50$ Hz, $k = 10$; $v_{\text{cr}} = 0.1$ m/sec; d = 72 μm , corundum; g_k and U are in percent.

TABLE 2. Experimental Materials

Material	Mixture number				
	1	2	3	4 ^{*)}	5 ^{*)}
Fine fraction $d_f, \mu\text{m}$	Corundum 72	Corundum 72	Corundum 72	Corundum 57	Corundum 140
Coarse fraction $d_c, \mu\text{m}$	Corundum 225	Corundum 358	Corundum 515	Alundum 5500	Alundum 5500

*Data on the effect of dispersed coarse additives on the resonance in a dispersed, fine, vibration-liquefied bed [21].

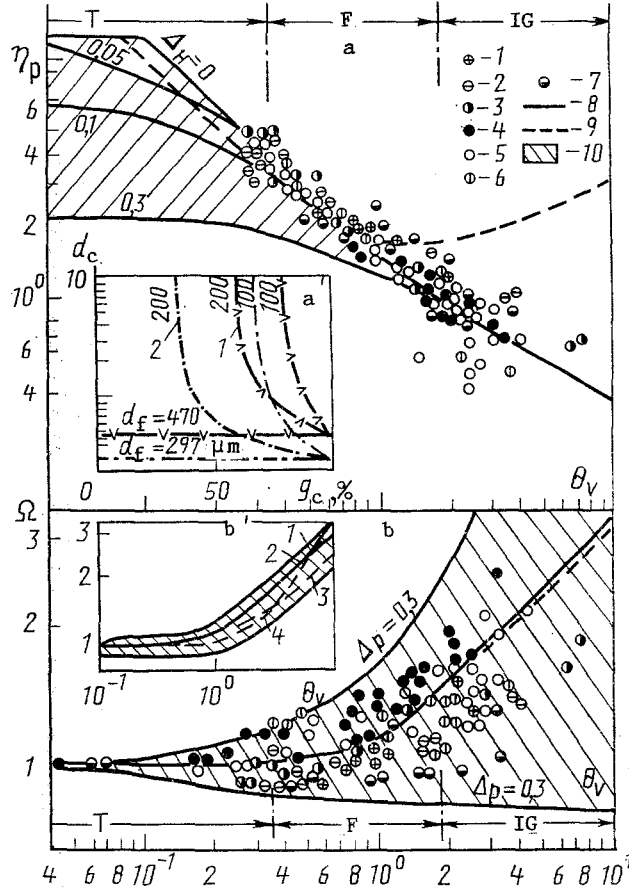


Fig. 3. Resonant pressures (a) and frequencies (b) of the vibration-liquefaction of charges: 1-3) mixtures 1-3 in Table 2; 4) mixtures 4 and 5; 5) $d = 72 \mu\text{m}$, $U = 0.5-10\%$; 6) data from [13]; 7) data from [22]; 8, 9) calculations from (8) and (9); 10) region with $\Delta H, \Delta p \leq 0.3$; a') lines $\theta_v = 10$ for binary mixtures: 1) 20 Hz; 2) 50 Hz; b': 1) Ω_p ; 2) $(\pi/4)(\eta_p \theta_v)$; 3) a_p/a_0 ; 4) a_{gr}/a_0 ; shaded region shows maximum values of structural, hydrodynamic and mass-transfer characteristics in the vibrating layer from data of various investigators [23]; $d, \mu\text{m}$.

coarsening of the mixture $d^* > d$ (the calculated curves in Fig. 2a). The decrease in the calculations from (8) relative to the experiment observed (Fig. 2a) in the region $g_c \approx 40-50\%$ can be explained as both an increase of the role of the coarse fraction in (3) and the plastic (shock) component of the pressure, which is significant here, but is not considered in the model (8), (9).

In a moist bed, the resonant pressure pulsations are minimal in the region of the largest granule porosity that is connected to the interparticle space ($U \approx 1.5\%$) and increases as the moisture content increases. This change is accompanied by an increase of the density of the granules without changing their dimensions significantly (Fig. 2b).

In the aerated layer the pressure pulsations change according to the change in porosity (Fig. 2c).

When the data in Fig. 2 are plotted in dimensionless coordinates, there is good agreement between calculations and experiments in the region of vibration-liquefaction of finely and thinly dispersed charges ($\theta_v < 1.7$) and an increase in the scatter of the pressure data when the material is processed, as compared to the effective characteristics for intermediate and large-grained materials. Here the experimental frequencies are within $\pm 30\%$ of the calculated resonance. In conclusion, we note that in calculating pressure pulsations from the rheodynamic model (9), the proposed approach is suitable for frequencies θ_v up to 1.7, but in calculating the frequencies, the applicability of the approach expands to the upper physical bound for the existence of resonant vibration-liquefaction regimes of $\theta_v \approx 10$, as described by the continuum model (8). Here the grains of the coarse fraction in the mixture can be related to lumped (spherical) materials (Fig. 3a).

Engineering calculations of the pressure pulsations for $\theta_v = 1.7-10$ can be conducted using the approximation

$$\eta_p' \theta_v = \frac{4}{\pi} \Omega_H', \quad (10)$$

which for $\theta_v < 1/\pi$ transforms to the invariant $\eta_p' \theta_v = 4/\pi$ (Fig. 3b). Here the resonant frequency Ω_H' can be determined in the acoustic approximation by [23]

$$\omega \simeq \pi a_\phi / (2H), \quad (11)$$

where $a_\phi = a_0 \sqrt{1 + \sqrt{1 + \theta_v^2}} / \sqrt{2}$ is the phase velocity of sound in the heterogeneous medium, which is obtained [17, 24] by solving (8).

NOTATION

A) amplitude; a) sound speed; c) volumetric concentration; D) granule diameter; d) particle diameter; f) frequency; g) acceleration due to gravity or mass concentration; H) height; k) acceleration; M) specific mass of the bed; P) total pressure; p) pressure deviation from the average; S) gas trajectory during a vibration half-period; t) time; U) moisture content in the total mass of the bed; v) gas velocity; v_t) terminal velocity of gas; W) fluidization number; X) average bed deformation; α) permeability coefficient; ϵ) porosity; η_p) dimensionless pressure; θ_v) dimensionless vibration frequency; μ) dynamic viscosity of the gas; ρ) density; τ) volume density; τ_v) velocity relaxation time of the phases; Ω) relative frequency; ω) angular frequency. Indices: g) gas; l) liquid; c) coarse; cr) critical; f) fine; 0) initial, average, or equilibrium; tot) total; b) fluidized bed; ϕ) phase; p) particle. Symbols: $D_t = \partial/\partial t$; $D_x = \partial/\partial x$; dimensionless and dimensional groups: $a_0^2 = P_0/(\rho_b \epsilon)$; $k = Aw^2/g$; $\Delta_H = 1 - \Omega_H/\Omega_H'$; $\Delta p = 1 - \eta_p/\eta_p'$; $\theta_v = \omega \tau_v$; $\Omega = \omega/\omega_0^*$.

LITERATURE CITED

1. K. Erdesz and A. S. Mujumdar, *Powder Technol.*, **46**, 167-172 (1986).
2. V. A. Chlenov and N. V. Mikhailov, *The Vibration-Fluidized Bed* [in Russian], Moscow (1972).
3. V. I. Mushtaev and V. S. Ul'yanov, *Drying Dispersed Materials* [in Russian], Moscow (1988).
4. A. P. Baskakov, A. F. Ryzhkov, A. S. Kolpakov, et al., III Ogolnopolski Symposjon Termodynamika Waretwy Fluidalnej [in Polish], Czestochowa (1985), pp. 17-23.
5. A. I. Tamarin and G. M. Kovenskiĭ, *Teor. Osn. Khim. Tekh.*, **6**, No. 1, 83-86 (1972).
6. A. F. Ryzhkov, A. S. Kolpakov, A. K. Barakyan, et al., *Heat and Mass Transfer in Industrial Processes and Equipment* [in Russian], Minsk (1985), pp. 119-126.
7. B. A. Putrik, A. S. Kolpakov, A. F. Ryzhkov, et al., *Thermal Physics of Nuclear Power Plants* [in Russian], Sverdlovsk (1985), pp. 76-82.
8. S. M. P. Mutser, K. Reitema, *Powder Technol.*, **24**, No. 1, 57-63 (1979).
9. N. I. Syromyatnikov and V. F. Volkov, *Processes in a Fluidized Bed* [in Russian], Sverdlovsk (1959).
10. A. S. Kolpakov, A. F. Ryzhkov, A. V. Pavlichenko, et al., Ural Polytechnic Institute, Sverdlovsk (1980); Dep. No. 91-80 in (GOSINTI) State Scientific Research Institute of Scientific and Technical Information (1980).

11. A. V. Blinov, B. G. Sapozhnikov, and N. I. Syromyatnikov, Heat and Mass Transfer in Industrial Processes and Equipment [in Russian], Minsk (1985), pp. 93-98.
12. A. F. Ryzhkov, I. É. Kipnis, and A. P. Baskakov, Inzh.-fiz. Zh., 60, No. 2, 209-217 (1991).
13. I. É. Kipnis, A. F. Ryzhkov, A. S. Kolpakov, et al., Thermal Physics of Nuclear Power Plants [in Russian], Sverdlovsk (1987), pp. 68-77.
14. A. P. Baskakov, B. V. Berg, A. F. Ryzhkov, et al., Processes of Heat and Mass Transfer in a Fluidized Bed [in Russian], Moscow (1978).
15. A. F. Ryzhkov and V. A. Mikula, Inzh.-fiz. Zh., 61, No. 1, 112-116 (1991).
16. N. I. Gel'perin, V. G. Aínshteín, and V. B. Kvasha, Basic Technology of Fluidization [in Russian], Moscow (1967).
17. A. F. Ryzhkov and B. A. Putrik, Inzh.-fiz. Zh., 54, No. 2, 188-197 (1988).
18. D. D. Barkan, Vibration Methods in Construction [in Russian], Moscow (1959).
19. W. Baader, Grundlagen des Landtechnik, No. 13, 13-20 (1961).
20. R. N. Volik, Problems of Separating Grains and Other Bulk Materials [in Russian], Moscow (1963), pp. 77-90.
21. A. S. Kolpakov, "Intensitification of heat and mass transfer in a layer of finely dispersed particles by vibration-liquefaction in resonance regimes," Dissertation for candidate of technical sciences [in Russian], Sverdlovsk (1983).
22. B. A. Putrik, "Optimization of thermal and hydrodynamic regimes in conductive equipment with a vibration-fluidized bed," Dissertation for candidate of technical sciences [in Russian], Sverdlovsk (1986).
23. A. F. Ryzhkov and E. M. Tolmachev, Teor. Osn. Khim. Tekh., 17, No. 2, 206-213 (1983).
24. V. L. Gapontsev, "Investigation of the formation mechanism and heat transfer in a vibration-fluidized bed with a vertical surface submersed in it," Dissertation for candidate of technical sciences [in Russian], Sverdlovsk (1981).
25. I. P. Mukhlenov, B. S. Sazhin, and V. F. Frolov (eds.), Handbook for Calculations of Fluidized-Bed Equipment [in Russian], Leningrad (1986).

NONSTATIONARY ISOTHERMAL EVAPORATION OF FLUIDS IN A CYLINDRICAL CHAMBER

Yu. G. Izmailov, E. A. Utkin, and G. P. Vyatkin

UDC 532.72;669.015.23

Numerical models for nonstationary isothermal evaporation of fluids in the cylindrical chamber of an experimental device are studied. The effect on the evaporation rate of the radii of the source and the output orifice is investigated. The relaxation times and the specific mass flux of the vapor are determined. The results are compared with analytic solutions for two limiting cases: the one-dimensional case and an infinite half-space.

The laws of mass transfer during the evaporation of solutions and melts of various types are of interest both industrially and ecologically. The most widely used information is on the temperature and concentration dependence of the evaporation rates, equilibrium partial pressures, and diffusion coefficients in gases [1, 2]. Much less attention is paid to investigating the effect of the configuration and geometric parameters of the equipment on the kinetic characteristics of the process.

Here we study the dependence of evaporation rates (average mass fluxes) on the dimensions of the liquid surface and the output orifice of a cylindrical chamber that is widely used

Chelyabinsk Polytechnic Institute. Translated from Inzhenerno-fizicheskii Zhurnal, Vol. 61, No. 5, pp. 790-794, November, 1991. Original article submitted February 4, 1991.